



## Deglacial landscapes and the Late Upper Palaeolithic of Switzerland

Hazel Reade<sup>a,\*</sup>, Jennifer A. Tripp<sup>a,1</sup>, Sophy Charlton<sup>b,2</sup>, Sonja B. Grimm<sup>a,c</sup>,  
Denise Leesch<sup>d</sup>, Werner Müller<sup>d</sup>, Kerry L. Sayle<sup>e</sup>, Alex Fensome<sup>a</sup>, Thomas F.G. Higham<sup>f</sup>,  
Ian Barnes<sup>b</sup>, Rhiannon E. Stevens<sup>a</sup>

<sup>a</sup> UCL Institute of Archaeology, 31-34 Gordon Square, London, WC1H 0PY, United Kingdom

<sup>b</sup> Department of Earth Sciences, Natural History Museum, Cromwell Road, London SW7 5BD, United Kingdom

<sup>c</sup> Centre for Baltic and Scandinavian Archaeology (ZBSA), Foundation Schleswig-Holsteinian State Museums Schloss Gottorf, Schlossinsel 1, 24837, Schleswig, Germany

<sup>d</sup> Université de Neuchâtel, Laboratoire d'archéozoologie, Avenue de Bellevaux 51, CH-2000, Neuchâtel, Switzerland

<sup>e</sup> Scottish Universities Environmental Research Centre, Rankine Avenue, East Kilbride, G75 0QF, United Kingdom

<sup>f</sup> Research Laboratory for Archaeology and the History of Art, University of Oxford, Dyson Perrins Building, South Parks Road, Oxford, OX1 3QY, United Kingdom

### ARTICLE INFO

#### Article history:

Received 17 January 2020

Received in revised form

1 May 2020

Accepted 15 May 2020

Available online xxx

#### Keywords:

Magdalenian

Collagen

Sulphur isotopes

Nitrogen isotopes

Carbon isotopes

Pleistocene

Palaeogeography

Europe

Horse

Reindeer

### ABSTRACT

The presence of people in Switzerland in recently deglaciated landscapes after the Last Glacial Maximum represents human utilisation of newly available environments. Understanding these landscapes and the resources available to the people who exploited them is key to understanding not only Late Upper Palaeolithic settlement in Switzerland, but more broadly human behavioural ecology in newly inhabited environmental settings. By applying bone collagen stable isotope analysis ( $\delta^{13}\text{C}$ ,  $\delta^{15}\text{N}$  and  $\delta^{34}\text{S}$ ) to faunal remains from Late Upper Palaeolithic localities in Switzerland, we investigate animal ecology and environmental conditions during periods of human occupation. High and relatively uniform  $\delta^{34}\text{S}$  values indicate that landscapes north of the Jura Mountains provided comparatively stable environmental conditions, while lower and more variable  $\delta^{34}\text{S}$  values on the Swiss Plateau suggest a dynamic landscape with diverse hydrological and pedological conditions, potentially linked to regionally different patterns of permafrost thaw. This contrasts with the archaeological record that appears relatively uniform between the two regions, suggesting people were employing similar subsistence behaviours across a range of environmental settings. The pattern of change in  $\delta^{15}\text{N}$  across the deglacial period appears consistent between areas that remained ice-free throughout the LGM and those that were glaciated. Most notable is a period of exclusively low  $\delta^{15}\text{N}$  values between 15,200 and 14,800 cal. BP, which could relate a regional expansion of floral biomass in response to environmental change.

© 2020 Elsevier Ltd. All rights reserved.

### 1. Introduction

The period after the Last Glacial Maximum (LGM) in Switzerland saw significant expansion of human settlement into previously ice-covered landscapes. This was facilitated by the rapid development of pioneer floral and faunal communities, and most likely by changes in the range dynamics of key prey species, such as horse

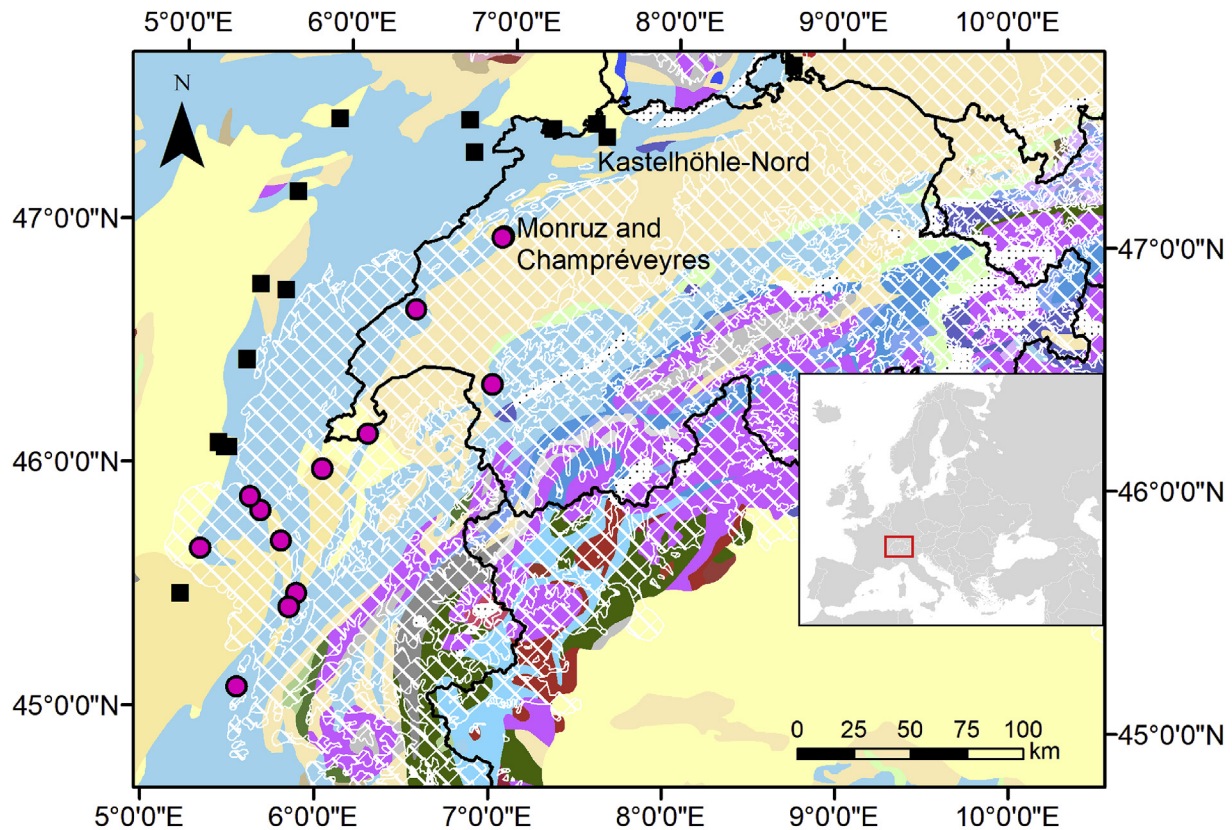
(*Equus* sp.) and reindeer (*Rangifer tarandus*) (Leesch et al., 2012; Cupillard et al., 2015). Understanding the environmental developments that drove such changes is key to interpreting the subsistence and settlement patterns of the human populations in this region and, more broadly, to investigating human behavioural ecology in newly available landscapes. Here we examine post-LGM paleoenvironmental conditions at two archaeological localities; Kastelhöhle-Nord (Fig. 1), which is situated north of the Jura Mountains and remained ice-free throughout the LGM, and Monruz and Champréveyres (Fig. 1), which are situated on the Swiss Plateau and became ice-free before 17,500 cal. BP (Ivy-Ochs et al., 2004). Bone collagen stable isotope analyses ( $\delta^{13}\text{C}$ ,  $\delta^{15}\text{N}$ , and  $\delta^{34}\text{S}$ ) are applied to the archaeological faunal assemblages from these sites to provide a direct record of past prey species ecology and

\* Corresponding author.

E-mail address: [h.reade@ucl.ac.uk](mailto:h.reade@ucl.ac.uk) (H. Reade).

<sup>1</sup> Department of Chemistry, University of San Francisco, 2130 Fulton Street, San Francisco, CA 94117, USA.

<sup>2</sup> PalaeoBARN, School of Archaeology, 1 South Parks Road, Oxford, OX1 3TG, United Kingdom.



### Bedrock geology

amphibolite	granite	meta-sediment group	sand
basalt	granulite	mica schist	sandstone
carbonates, consolidated	gravel	migmatite/anatexite	shale/slate
clay	greenschist	mudstone	siltstone
claystone	limestone	phyllite	syenite
conglomerate	marble	plutonic ultramafic group	tholeiitic basalt
diorite	marlstone	quartzite	tonalite
dolomite/dolostone	meta-rhyolite group	rhyodacite	undifferentiated
gneiss	meta-sandstone	rhyolite	

**Fig. 1.** Map showing the location of Monruz, Champréveyres and Kastelhöhle-Nord. Bedrock geology is from the International Geological Map of Europe (IGME 5000; [Asch, 2005](#)). Black line indicates present day country borders. White hatching indicates reconstructed limits of Last Glacial Maximum (LGM) ice sheet extent from [Becker et al. \(2015\)](#). Symbols indicate archaeological sites from which isotopic data used in our discussion comes (full data in Supplementary Information 5), from areas that were covered by ice at the LGM (pink circles) and those in areas that remained ice free throughout the LGM (black squares). Inset: location of Switzerland in Europe indicated by red box. (For interpretation of the references to colour in this figure legend, the reader is referred to the Web version of this article.)

environmental conditions during the period of human activity. New radiocarbon dates are also obtained from the fauna to better contextualise the chronology of human occupation. By combining this data with other published results, the pattern of post-LGM environmental change is compared between regions that remained ice-free throughout the LGM and those that were glaciated.

#### 1.1. Post-LGM environment and archaeology in Switzerland

Switzerland during the LGM was almost entirely covered by ice

with only a small region north of the Jura Mountains remaining unglaciated ([Ivy-Ochs et al., 2004](#); [Bini et al., 2009](#); [Ivy-Ochs, 2015](#)). While a brief phase of human occupation during the LGM occurred in the ice-free region ([Terberger and Street, 2002](#); [Reade et al., 2020](#)), it is not until after the LGM that evidence of widespread and sustained Late Upper Palaeolithic human activity becomes apparent ([Leesch et al., 2012](#)). Post-LGM ice sheet decay in Switzerland was rapid, and the entire central Swiss Plateau was ice free before the onset of Greenland Stadial 2.1a (GS-2.1a, c.17,450–14,650 BP, [Fig. 2](#); [Ivy-Ochs et al., 2004](#); [Rasmussen et al., 2014](#)). The exposure of new landscapes during Greenland Stadial

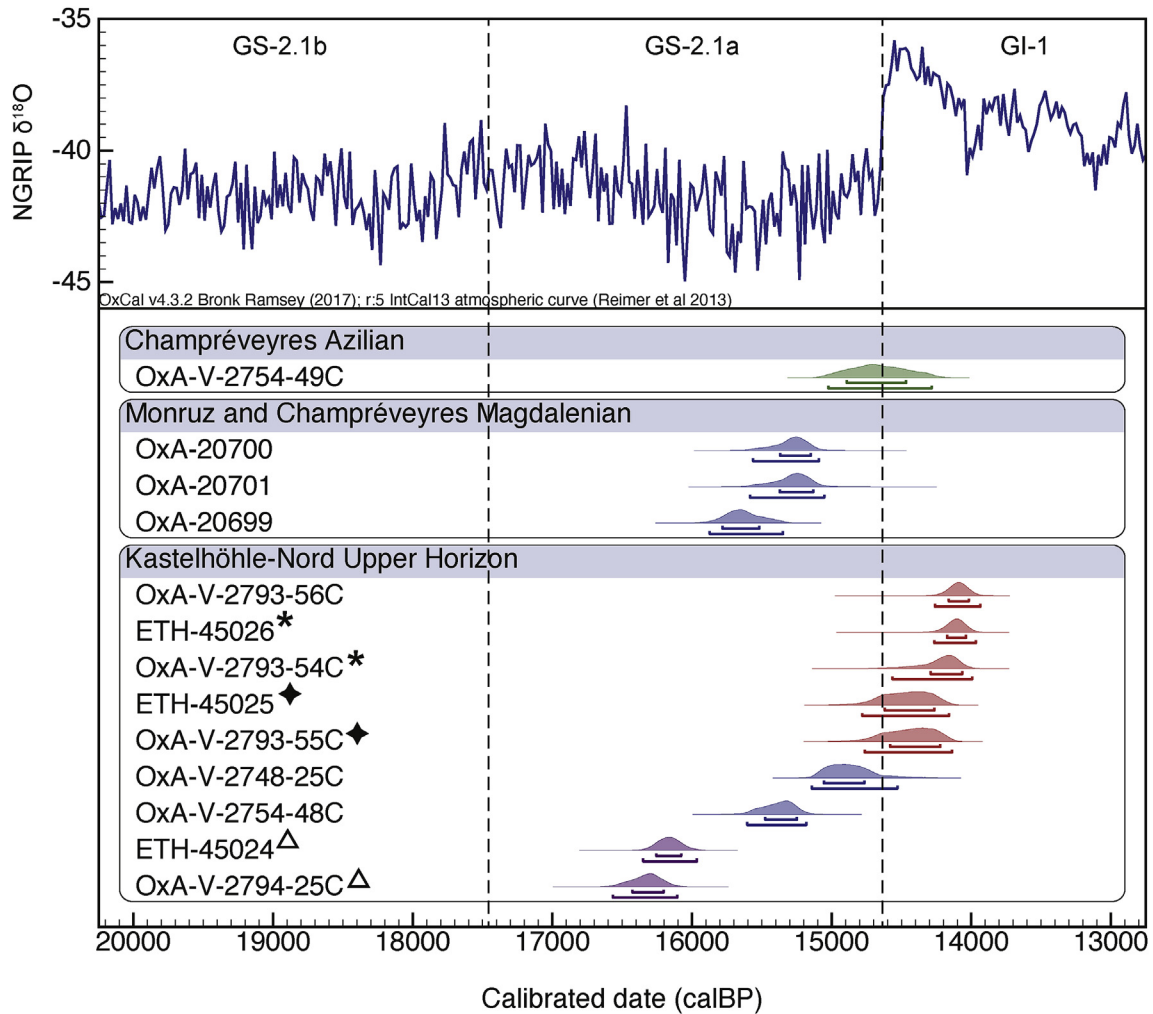


**Fig. 2.** Calibrated AMS radiocarbon determinations on faunal bone collagen from sites discussed in the text. Calibration was performed using OxCal 4.3 (Bronk Ramsey, 2017) and the INTCAL13 dataset (Reimer et al., 2013) and plotted with the Last Glacial period INTIMATE event stratigraphy and NGRIP ice core  $\delta^{18}\text{O}$  values (top; North Greenland Ice Core Project members, 2004; Rasmussen et al., 2014). Purple = *Bos/Bison*, blue = horse, red = reindeer, green = red deer. Kastelhöhle-Nord dates from this study (OxA codes) and Leesch and Müller (2012; ETH codes); Monruz and Champréveyres Magdalenian dates from Bodu (2009); Champréveyres Azilian dates from this study. Symbols \*, \*, and  $\Delta$  indicate date is on same bone specimen. (For interpretation of the references to colour in this figure legend, the reader is referred to the Web version of this article.)

2.1b (GS-2.1b, c. 20,850 to 17,450 BP, Fig. 2; Rasmussen et al., 2014) was quickly followed by the development of pioneer floral communities. Vegetation on the northern margins of the Jura Mountains was dominated by *Poaceae*, *Artemisia*, *Juniperus* and *Hippophae* (Cupillard et al., 2015), while species-rich treeless steppe tundra had developed on the Swiss Plateau by around 18,700 cal. BP (Rey et al., 2017). This was followed by an increase in herbaceous vegetation (e.g. Ammann and Lotter, 1989; Lotter, 1999; Wehrli et al., 2007) that allowed large herbivores to recolonise deglaciated regions by around 17,000 cal. BP (Morel and Hug, 1996; Hajdas et al., 2007).

There is some evidence for a relatively early phase of post-LGM human activity early in GS-2.1a, but the main expansion of settlement in Switzerland did not occur until the latter part of GS-2.1a (Weniger, 1989; Napierala, 2008; Leesch et al., 2012; Maier, 2015). These sites, associated with the Magdalenian culture, are characterised by a dominance of horse and reindeer in their faunal assemblages (Leesch et al., 2012; Nielsen, 2013; Maier, 2015). Attributed to Magdalenian techno-complexes D and E, the sites cover a wide geographic distribution across the Swiss Plateau and Jura region, indicating the exploitation of a variety of landscapes

(Leesch et al., 2012). Archaeological evidence comes from both caves and rockshelters, such as at Kesslerloch and Kastelhöhle-Nord, and open-air localities, such as the sites of Monruz and Champréveyres (Leesch et al., 2019). Coleoptera-based temperature estimates suggest summer and winter mean air temperatures on the Swiss Plateau during GS-2.1a were around 9 °C and -20 °C respectively (Coope and Elias, 2000; Thew et al., 2009), while summer temperatures of around 12 °C are estimated for the region north of the Jura mountains (Cupillard et al., 2015). Pollen and plant macrofossil evidence attest to vegetation rapidly increasing in diversity, but still dominated by cold-tolerant herbaceous species (Thew et al., 2009; Cupillard et al., 2015).

The onset of Greenland Interstadial 1 (GI-1, c. 14,650 to 12,850 BP, Fig. 2; Rasmussen et al., 2014) corresponds to a rapid rise in temperatures on the Swiss Plateau and the expansion of juniper and birch vegetation into open shrub and grasslands (Thew et al., 2009). It is currently not clear whether Magdalenian activity continued into this early phase of GI-1e or ended with the onset of this warm period, but by c. 14,400 cal. BP Azilian occupation of the Swiss Plateau was established (Leesch et al., 2012). During this time, mean summer and winter temperatures are estimated to have

been around 15 °C and 0 °C respectively, with vegetation composed of a mosaic of open birch woodland, patches of dwarf birch and shrubs, and areas of grasses and sedges (Leesch, 1997; Thew et al., 2009). These more temperate conditions are reflected in the change in subsistence focus, with red deer (*Cervus elaphus*) and horse being important prey species (Leesch et al., 2004; Nielsen, 2013; Maier, 2015).

Considering the availability of different prey species and the ecologies and environments they represent is key to understanding the landscapes past people would have experienced. Whilst there is a wealth of Swiss Lateglacial palaeoenvironmental data from numerous lake and mire archives (e.g. Lotter, 1999; Coope and Elias, 2000; Wehrli et al., 2007; Lotter et al., 2012; Cupillard et al., 2015; Rey et al., 2017), analysis of the archaeological faunal assemblage provides the means to directly link inferences on habitat, ecology, and palaeoenvironmental conditions, to human hunting, settlement and subsistence practices.

### 1.2. Palaeoenvironmental records from faunal stable isotopes

Palaeoenvironmental and ecological data can be obtained directly from skeletal remains of prey species from archaeological contexts through stable isotope analyses (e.g. Stevens and Hedges, 2004; Stevens et al., 2008, 2014; Drucker et al., 2011a, 2011b; 2012; Bocherens et al., 2015; Jones et al., 2018; Reade et al., 2020). In this study we use carbon ( $\delta^{13}\text{C}$ ), nitrogen ( $\delta^{15}\text{N}$ ) and sulphur ( $\delta^{34}\text{S}$ ) isotope ratios in bone collagen to explore post-LGM environments and prey species ecology in Switzerland. The measured isotopic signals are underpinned by dietary specialisation, animal behaviour and environmental conditions.

Bone collagen  $\delta^{13}\text{C}$  values are largely determined by species-specific dietary behaviours, such as grazing versus browsing, or specific dietary specialisations, such as the consumption of lichens by reindeer, which leads to systematically higher  $\delta^{13}\text{C}$  values in comparison to other herbivore species (Drucker et al., 2010; Bocherens et al., 2015). However, dietary  $\delta^{13}\text{C}$  values also reflect atmospheric  $\text{CO}_2$  concentration and  $\delta^{13}\text{C}$ , environmental variables such as temperature and moisture availability, and vegetation density and type (Heaton, 1999; Stevens and Hedges, 2004; Drucker et al., 2008; Kohn, 2010). Faunal  $\delta^{15}\text{N}$  values are linked to both dietary specialisation/niche position and to climatic parameters, such as temperature and precipitation, mediated through soil processes (Amundson et al., 2003; Stevens et al., 2008, 2014; Drucker et al., 2011b, 2012; 2018 Craine et al., 2015; Rabanus-Wallace et al., 2017). In particular, nutrient availability and microbial activity may be reflected in herbivore bone collagen  $\delta^{15}\text{N}$  values, parameters that were likely strongly influenced by the presence of permafrost and ice sheets in the European Lateglacial (Stevens and Hedges, 2004; Stevens et al., 2008; Drucker et al., 2011b). Collagen  $\delta^{34}\text{S}$  values relate to the soil environment upon which the animal fed. Bioavailable sulphur can be derived from sulphates in groundwater and rain, atmospheric sulphur, and from mineral weathering of the underlying geology (Nehlich, 2015). As such, bone collagen  $\delta^{34}\text{S}$  values are spatially variable and often considered a tool for exploring mobility and landscape utilisation (e.g. Drucker et al., 2012, 2018; Jones et al., 2018; Wißing et al., 2019). However, bone collagen  $\delta^{34}\text{S}$  values may also hold significant promise as a palaeoenvironmental proxy, as soil-bedrock interactions, mineral weathering, and sulphur cycling in the soil are driven by hydrological and microbial processes (Thode, 1991). These are dynamic systems influenced by climatic and environmental conditions, such that  $\delta^{34}\text{S}$  values in the local landscape are unlikely to have remained static across major environmental transitions, for example the last deglaciation.

## 2. Materials and methods

In this study we present  $\delta^{13}\text{C}$ ,  $\delta^{15}\text{N}$  and  $\delta^{34}\text{S}$  data generated from horse, reindeer, red deer and *Bos/Bison* bone collagen samples from the Swiss sites of Kastelhöhle-Nord, Monruz and Champréveyres to explore animal ecology and environmental conditions after the LGM.

### 2.1. Archaeological samples

The faunal assemblage from Kastelhöhle-Nord provides a record from the ice-free region of Switzerland, on the north edge of the Jura Mountains. Excavation of the cave between 1948 and 1954 revealed an 'intermediate' horizon associated with a Badegoulian phase of occupation, dated to the latter part of the LGM (Terberger and Street, 2002; Reade et al., 2020), and a 25 cm-thick 'upper' horizon associated with the post-LGM Magdalenian (Leesch et al., 2012). This upper horizon contained a rich lithic assemblage that certainly represents more than one phase of Magdalenian activity at the site and most likely comprises more than one techno-complex (Magdalenian D-a and E; Leesch et al., 2012). A relatively long duration of accumulation for this horizon was confirmed by three faunal radiocarbon dates, which range from 16,350–15,965 cal. BP (ETH-45024) to 14,265–13,967 cal. BP (ETH-45026) (Leesch et al., 2012, Fig. 2, Table 1). We sampled the large herbivore species found within the upper horizon (Schweizer et al., 1959); reindeer ( $n = 10$ ), horse ( $n = 5$ ) and *Bos/Bison* ( $n = 6$ ). Of these, one reindeer bone displayed evidence of anthropogenic impact (cut marks). To investigate the chronology of this horizon, 3 specimens (two horse and the cut-marked reindeer bone) were selected for radiocarbon dating. The three specimens that had previously been dated (two reindeer, one *Bos/Bison*) were also re-dated to ensure methodological consistency between laboratories.

Comparative post-LGM samples from the Swiss Plateau, which was glaciated during the LGM, come from the open-air localities of Monruz and Champréveyres. Excavated between 1984 and 1992, both sites produced Late Upper Palaeolithic Magdalenian and Azilian occupation horizons, with rich faunal, botanical and lithic assemblages. Phases of Magdalenian activity at the sites date to the later part of GS-2.1a and were focused primarily on the exploitation of horse, together with a broad spectrum of smaller mammals, birds and fish, particularly in spring and summer (Müller et al., 2006; Müller, 2013). Three horse bones from these assemblages have previously been radiocarbon dated, producing age determinations between 15,874–15,349 cal. BP (OxA-20699) and 15,585–15,053 cal. BP (OxA-20701) (Fig. 2, Table 1). We selected five reindeer and 12 horse samples from Monruz (all from Magdalenian sector 1) and 7 red deer samples from Champréveyres (four from Magdalenian sector 2, two from Azilian sector 1, and one from sector 2 where the association to the Magdalenian or Azilian was uncertain) for stable isotope analysis. While the specimens do not bear direct traces of anthropogenic action, the large herbivore faunal assemblage from the sites is confidently interpreted as the product of human action (Müller et al., 2006; Müller, 2013). While Magdalenian activity has been dated both from faunal and charcoal remains, dating of the Azilian phase has so far relied solely on charcoal samples. Therefore, one bone from the Azilian concentration at Champréveyres was selected for radiocarbon dating as part of this study.

### 2.2. Sample pre-treatment

A small sample of bone (0.2–1.3g) was collected from each specimen using a dental drill with either a small cutting wheel or tungsten burr attachment. Samples were prepared at University

**Table 1**

AMS radiocarbon determinations on bone collagen from the sites and levels discussed in the text, and as shown in Fig. 2  $\delta^{13}\text{C}$  and C/N ratio measured by IRMS as part of the radiocarbon dating procedure at the Oxford Radiocarbon Accelerator Unit. Calibration of radiocarbon age determinations was performed using OxCal 4.3 (Bronk Ramsey, 2017) and the INTCAL13 dataset (Reimer et al., 2013). References (Ref) for dates: <sup>1</sup>this study; <sup>2</sup>Leesch and Müller (2012); and <sup>3</sup>Bodu et al. (2009).

Project sample code	Species	Element	Collagen yield (%)	$\delta^{13}\text{C}$ (‰)	C/N ratio	AMS Code	<sup>14</sup> C BP	Calibrated Age BP (2 $\sigma$ )	Time Period	Ref
Kastelhöhle-Nord, upper horizon										
UPN-232	<i>Bos/Bison</i>	metacarpus	10.4	-19.5	3.3	OxA-V-2794-25C	13,550 ± 60	16,566–16,107	GS-2.1a	1
			not given	-18.8	not given	ETH-45024	13,435 ± 50	16,350–15,965	GS-2.1a	2
UPN-214	<i>Equus</i> sp.	phalanx I	2.8	-21.1	3.2	OxA-V-2754-48C	12,880 ± 50	15,605–15,181	GS-2.1a	1
UPN-218	<i>Equus</i> sp.	carpal	8.1	-20.4	3.2	OxA-V-2748-25C	12,560 ± 50	15,142–14,529	GS-2.1a/GI-1e	1
UPN-212	<i>Rangifer tarandus</i>	tibia	5.4	-19.6	3.3	OxA-V-2793-55C	12,380 ± 50	14,764–14,138	GI-1ed	1
			not given	-18.9	not given	ETH-45025	12,395 ± 45	14,780–14,160	GI-1ed	2
UPN-204	<i>Rangifer tarandus</i>	radius	7.4	-19.5	3.3	OxA-V-2793-54C	12,270 ± 60	14,740–14,129	GI-1ed	1
			not given	-19.8	not given	ETH-45026	12,215 ± 45	14,265–13,967	GI-1ed	2
UPN-213	<i>Rangifer tarandus</i>	tibia, cut-marked	4.5	-19.6	3.4	OxA-V-2793-56C	12,200 ± 50	14,260–13,935	GI-1ed	1
Monruz and Champréveyres Magdalenian										
n/a	<i>Equus</i> sp.	femur	not given	-20.3	not given	OxA-20699	13,055 ± 60	15,874–15,349	GS-2.1a	3
n/a	<i>Equus</i> sp.	talus	not given	-20.5	not given	OxA-20700	12,815 ± 65	15,562–15,092	GS-2.1a	3
n/a	<i>Equus</i> sp.	talus	not given	-20.4	not given	OxA-20701	12,805 ± 75	15,585–15,053	GS-2.1a	3
Champréveyres Early Azilian										
UPN-240	<i>Cervus elaphus</i>	metatarsal	2.3	-20.9	3.3	OxA-V-2754-49	12,480 ± 50	15,023–14,284	GS-2.1a/GI-1e	1

College London (UCL) using a modified version of the Oxford Radiocarbon Accelerator Unit (ORAU) collagen extraction procedures (AF and AG methods; Brock et al., 2010), which is based on a modified version of the Longin (1971) method. All samples were treated with 0.5M hydrochloric acid (HCl) at 4 °C until fully demineralised and then thoroughly rinsed with ultrapure water. Some samples were then also treated with 0.1M sodium hydroxide (30mins), and 0.5M HCl (1hr) to remove humic contaminants (Szpak et al., 2017), again being thoroughly rinsed with ultrapure water between reagents. All samples were then gelatinised in pH3 HCl solution at 75 °C for 48hrs and filtered using a pre-cleaned Ezeeb-filter. For most samples, including all those to be radiocarbon dated, the filtrate was then passed through a pre-cleaned 15–30 kD ultrafilter, with the >30 kD fraction collected and freeze-dried (AF method). For some samples the ultrafiltration step was omitted (AG method); while ultrafiltration has been shown to successfully improve the removal of contaminants that can influence radiocarbon determinations (Higham et al., 2006), it also significantly reduces collagen yield, while at the same time producing little difference in measured stable isotope compositions (Sealy et al., 2014; Szpak et al., 2017). Details of pre-treatment methodology are given for each sample in the supplementary information S1.

### 2.3. Stable isotope analysis

Collagen yields from Kastelhöhle-Nord ranged from 2.3 to 16.2%. Collagen preservation at Monruz and Champréveyres was poorer; 12 out of 24 samples failed to produce enough collagen for stable isotope analysis (yields  $\leq 0.7\%$ ), while the other 12 samples had collagen yields ranging from 0.8 to 3.6% (supplementary information S1). Samples with adequate collagen were analysed for their nitrogen ( $\delta^{15}\text{N}$ ), carbon ( $\delta^{13}\text{C}$ ), and sulphur ( $\delta^{34}\text{S}$ ) isotopic ratios at the Scottish Universities Environmental Research Centre (SUERC). 1.2–1.5 mg aliquots of freeze-dried collagen were weighed into tin capsules and analysed using a Delta V Advantage continuous-flow isotope ratio mass spectrometer coupled via a ConFloIV to an EA IsoLink elemental analyser (Thermo Fisher Scientific, Bremen). For every ten archaeological samples, three in-house standards, calibrated to the International Atomic Energy Agency (IAEA) reference materials, were analysed (Sayle et al., 2019). Results are reported as per mil (‰) relative to the internationally accepted standards VPDB, AIR and VCDT. Measurement uncertainty was determined to be

$\pm 0.1\%$  for  $\delta^{13}\text{C}$ ,  $\pm 0.2\%$  for  $\delta^{15}\text{N}$ , and  $\pm 0.3\%$  for  $\delta^{34}\text{S}$ , on the basis of repeated measurements of an in-house bone collagen standard and a certified fish gelatin standard (Elemental Microanalysis, UK). Standard quality control criteria were used to assess the  $\delta^{13}\text{C}$ ,  $\delta^{15}\text{N}$  and  $\delta^{34}\text{S}$  data (DeNiro, 1985; Ambrose, 1990; Nehlich and Richards, 2009). Each sample was analysed in duplicate and reproducibility was better than  $\pm 0.1\%$  for  $\delta^{13}\text{C}$ ,  $\pm 0.2\%$  for  $\delta^{15}\text{N}$  and  $\pm 0.3\%$  for  $\delta^{34}\text{S}$ . All analysed samples had C:N atomic ratios between 3.2 and 3.6, and %C and %N between 35–46% and 12–16%, respectively, indicating good bone collagen preservation (DeNiro, 1985; Ambrose, 1990). All analysed samples except UPN-240 had C:S and N:S atomic ratios within the recommended ranges of  $600 \pm 300$  and  $200 \pm 100$ , and %S content between 0.14 and 0.30% (Nehlich and Richards, 2009).

### 2.4. Radiocarbon analysis and background corrections

Radiocarbon dating was performed at ORAU using their standard procedures, as described by Brock et al. (2010). For each sample, approximately 5 mg of dry collagen, which had been weighed into tin capsules baked at 500 °C for 12 h, was combusted using an elemental analyser coupled to an isotope ratio mass spectrometer, employing a splitter to allow for collection of the  $\text{CO}_2$  (Bronk Ramsey and Humm, 2000; Brock et al., 2010). Samples were graphitised by reduction of collected  $\text{CO}_2$  over an iron catalyst in an excess  $\text{H}_2$  atmosphere at 560 °C (Bronk Ramsey and Hedges, 1997; Dee and Bronk Ramsey, 2000). <sup>14</sup>C dates were measured on the Oxford AMS system using a cesium ion source for ionisation of the solid graphite sample (Bronk Ramsey et al., 2004). To denote the bone pretreatment at UCL rather than at ORAU, all measured dates were given “OxA-V-wwww-pp” numbers, where wwwwww indicates the wheel number, and “pp” is the position of the sample on the wheel (Brock et al., 2010). As collagen extraction was performed at UCL according to the ORAU pretreatment protocol, background corrections were applied to our dates based on repeat AMS measurements at ORAU of known-aged reference samples prepared in the UCL laboratory, following the method outlined by Wood et al. (2010). A full description of our correction methodology is detailed in Reade et al. (2020). Corrected dates are denoted by adding a “C” to the end of the date code assigned by ORAU. Uncorrected measured date values as well as further details of the correction calculations are provided in the supplemental information S2.

### 3. Results and discussion

#### 3.1. Chronology of the lateglacial assemblage at Kastelhöhle-Nord and Champréveyres

Six new radiocarbon determinations were made on fauna from the upper horizon at Kastelhöhle-Nord (Fig. 2, Table 1). Three of these were undertaken on previously dated specimens for inter-laboratory comparison, and the results reflect those previously obtained (Leesch and Müller, 2012) (Table 1). The new dates for Kastelhöhle-Nord's upper horizon range from  $13,550 \pm 60$   $^{14}\text{C}$  BP (OxA-V-2794-25C) to  $12,200 \pm 50$   $^{14}\text{C}$  BP (OxA-V-2793-56C), giving a range of calibrated ages between 16,350–15,965 cal. BP and 14,260–13,935 cal. BP, further confirming an extended period of bone accumulation in the horizon. There appears to be a species-based chronological pattern to the results (Fig. 2); *Bos/Bison* and horse date to GS-2.1a and reindeer to GI-1. However, this finding is likely coincidental as reindeer dating to GS-2.1a are known at other sites within the same valley system (e.g. Hollenberg-Höhle 3; Müller and Leesch, 2011), as are horse dating to GI-1 (e.g. Kohlerhöhle; Leesch and Müller, 2012). Thus, both species were present within the local landscape at the same time as one another.

Archaeologically, the dating of a cut-marked reindeer bone found in association with Magdalenian artefacts to the later, colder part of GI-1ed is problematic when considered against our current understanding of the chronology of Magdalenian/Azilian development and their subsistence systems in the region. While it is recognised that the Kastelhöhle-Nord upper horizon lithic assemblage most probably represents more than one Magdalenian techno-assemblage (Leesch et al., 2012), the reindeer date is significantly later than those at other Magdalenian sites in the region and also later than dates associated with the Early Azilian assemblages at Monruz and Champréveyres. Therefore, it appears reindeer hunting at Kastelhöhle-Nord continued or resumed after the Magdalenian disappeared from the archaeological record in adjacent regions. As the bone was found in the mixed Magdalenian techno-assemblage the question arises whether this lithic tradition survived or was revived with the hunting of reindeer during GI-1ed, or whether there is a yet unrecognised lithic assemblage type admixed in the

upper horizon. Comparable late GI-1ed radiocarbon dates on faunal remains (horse, ptarmigans, red deer and dog) have come from the nearby cave of Büttenloch, and from other northern Swiss localities, namely Rislisberghöhle and Kesslerloch (Napierala, 2008; Leesch and Müller, 2012). Chronologically, the dates are compatible with the Azilian phase in Switzerland, although the dated fauna cannot be certainly attributed to the subsistence activities of this culture.

One new radiocarbon determination was made on a red deer bone from the Azilian horizon at Champréveyres, which had so far been chronologically constrained by radiocarbon determinations made on charcoal and macrobotanical remains (Leesch, 1997). The date,  $12,480 \pm 50$   $^{14}\text{C}$  years BP (OxA-V-2754-49C, Fig. 2, Table 1), falls within the range of dates on charcoal from hearth deposits, confirming the contemporaneity of the faunal assemblage with human activity at the site.

#### 3.2. Lateglacial ecology and environment at Kastelhöhle-Nord and Monruz/Champréveyres

Kastelhöhle-Nord upper horizon  $\delta^{13}\text{C}$  values overlap for reindeer and *Bos/Bison*, ( $-20.3\text{‰}$  to  $-19.4\text{‰}$  and  $-20.1\text{‰}$  to  $-19.7\text{‰}$ , respectively) while horse  $\delta^{13}\text{C}$  values differ ( $-21.3\text{‰}$  to  $-20.2\text{‰}$ ) (Fig. 3, Table 2). A similar offset between reindeer and *Bos/Bison*, and horse is also observed in the nitrogen isotope data, which ranges from  $0.7\text{‰}$  to  $2.3\text{‰}$  for horse, compared to  $2.3\text{‰}$ – $3.5\text{‰}$  and  $2.6\text{‰}$ – $4.0\text{‰}$  for reindeer and *Bos/Bison* respectively (Fig. 3, Table 2). The significant species-based differences between  $\delta^{13}\text{C}$  and  $\delta^{15}\text{N}$  values (Fig. 3, supplementary information S3.1 and S3.2) can largely be explained by species ecology and dietary specialisation. The comparable *Bos/Bison* and reindeer  $\delta^{13}\text{C}$  values indicate ecological overlap. Reindeer typically display higher  $\delta^{13}\text{C}$  values than other herbivore species due to lichen consumption; this dietary behaviour has also been observed in some modern bison populations and has previously been suggested for the species in other Late Pleistocene contexts (Larter and Gates, 1991; Julien et al., 2012; Bocherens et al., 2015). The two species also display similar  $\delta^{15}\text{N}$  and  $\delta^{34}\text{S}$  values (Fig. 3, Table 2), further supporting the interpretation of overlapping habitat preferences. Lower  $\delta^{13}\text{C}$  and  $\delta^{15}\text{N}$  values in horse compared to reindeer is a pattern that is observed

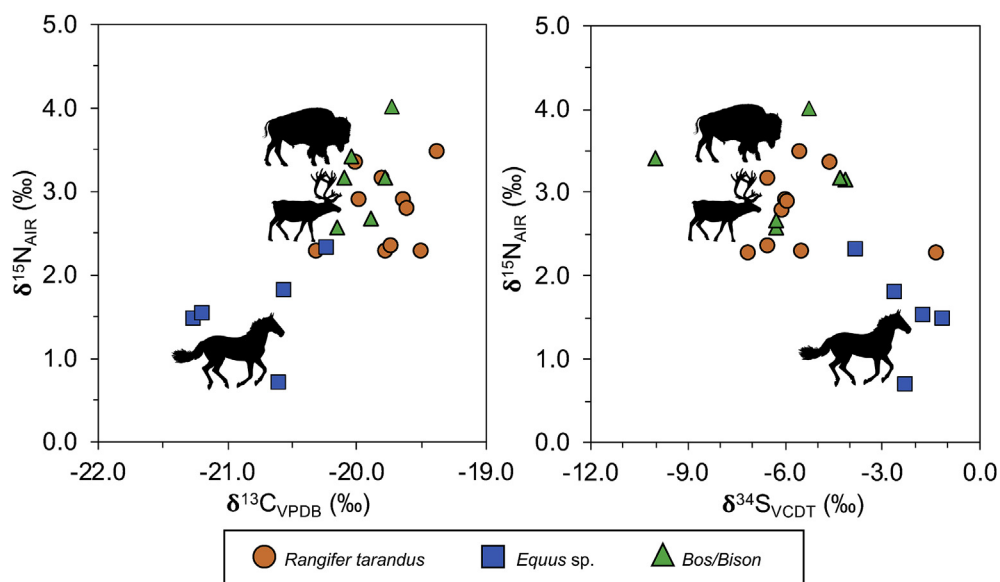


**Fig. 3.**  $\delta^{13}\text{C}$ ,  $\delta^{15}\text{N}$ , and  $\delta^{34}\text{S}$  values of Kastelhöhle-Nord upper horizon samples. Overlap in values can be seen between *Bos/Bison* (green triangles) and reindeer (*Rangifer tarandus*, orange circles), while horse (*Equus sp.*, blue squares) are dissimilar in their isotopic values. Enlarged symbols represent directly dated samples reported in Fig. 2. (For interpretation of the references to colour in this figure legend, the reader is referred to the Web version of this article.)

**Table 2**

Summary statistics for carbon, nitrogen and sulphur isotopic ratios for each species and archaeological site. Each sample was analysed in duplicated by IRMS at the Scottish Universities Environmental Research Centre. Data in ( ) was deemed unreliable based on standard quality control criteria. Full results are presented in the Supplementary Information 1.

Fauna	n	Average $\delta^{13}\text{C}$ (‰)	Max $\delta^{13}\text{C}$ (‰)	Min $\delta^{13}\text{C}$ (‰)	Average $\delta^{15}\text{N}$ (‰)	Max $\delta^{15}\text{N}$ (‰)	Min $\delta^{15}\text{N}$ (‰)	Average $\delta^{34}\text{S}$ (‰)	Max $\delta^{34}\text{S}$ (‰)	Min $\delta^{34}\text{S}$ (‰)
Kastelhöhle Nord, upper horizon										
<i>Bos/Bison</i>	6	$-19.9 \pm 0.2$	-19.7	-20.1	$3.2 \pm 0.5$	4.0	2.6	$-6.1 \pm 1.9$	-4.2	-10.0
<i>Equus</i> sp.	5	$-20.8 \pm 0.4$	-20.2	-21.3	$1.6 \pm 0.5$	2.3	0.7	$-2.3 \pm 0.9$	-1.2	-3.8
<i>Rangifer tarandus</i>	10	$-19.7 \pm 0.3$	-19.4	-20.3	$2.8 \pm 0.4$	3.5	2.3	$-5.5 \pm 1.5$	-1.3	-7.1
Monruz										
<i>Equus</i> sp.	7	$-21.0 \pm 0.2$	-20.8	-21.4	$1.8 \pm 0.6$	2.9	1.1	$-12.3 \pm 5.2$	-3.6	-19.8
<i>Rangifer tarandus</i>	4	$-19.8 \pm 0.2$	-19.6	-20.1	$2.8 \pm 0.2$	3.2	2.6	$-13.8 \pm 2.9$	-10.3	-17.3
Champréveyres										
<i>Cervus elaphus</i>	1	-20.7	-	-	2.4	-	-	(-7.2)	-	-

across Pleistocene Europe and indicates occupation of a different ecological niche (Stevens and Hedges, 2004; Stevens et al., 2008; Bocherens et al., 2015). The  $\delta^{34}\text{S}$  values observed for horse also differ from those of reindeer and *Bos/Bison* (Fig. 3, Table 2), further suggesting that the animals were not only occupying different niches, but also possibly different landscapes and/or different topographical features/locations within a given area. However, it should be noted that the species-dependent chronological pattern observed in the radiocarbon dates (Fig. 2) means that it cannot be certainly demonstrated that any of the individuals analysed here overlap in their chronology, and as such, the differences observed may partly be influenced by temporally changing underlying environmental parameters. Pollen records indicate the vegetation north of the Jura mountains was dominated by a mosaic of *Poaceae*, *Artemisia*, *Juniperus* and *Hippophae* species during GS-2.1a, with *Juniperus* and *Betula* expanding at the start of GI-1e, while climatic proxies suggest both an increase in temperature and precipitation across this time interval (Cupillard et al., 2015). Thus, the observed isotopic data likely represents a combined signal of environmental change and species-specific patterns of habitat utilisation.

A similar pattern of variation between horse and reindeer is seen in the Monruz results (Fig. 4). At this site average horse  $\delta^{15}\text{N}$  values ( $1.8 \pm 0.6\text{‰}$ ) and  $\delta^{13}\text{C}$  values ( $-21.0 \pm 0.2\text{‰}$ ) are significantly

different to the reindeer values ( $2.8 \pm 0.2\text{‰}$  and  $-19.8 \pm 0.2\text{‰}$ , respectively) (S3.3). Furthermore,  $\delta^{13}\text{C}$  and  $\delta^{15}\text{N}$  values for horse at Monruz and Kastelhöhle-Nord upper horizon are indistinguishable from one another; the same is also observed for reindeer from the two sites (S3.4 and S3.5). By contrast, horse and reindeer  $\delta^{34}\text{S}$  values at Monruz are statistically indistinguishable from one another (Fig. 4; S3.6), but significantly different to those of the horse and reindeer at Kastelhöhle-Nord (S3.7). Therefore,  $\delta^{13}\text{C}$  and  $\delta^{15}\text{N}$  values cluster by species, indicating that ecological niche and animal behaviour are the primary factors influencing these values, while  $\delta^{34}\text{S}$  values cluster by site, indicating that location-based factors are most strongly represented in the sulphur isotope ratios. Almost twice as much variability is observed in the Monruz  $\delta^{34}\text{S}$  values (16.5‰) than in the Kastelhöhle-Nord  $\delta^{34}\text{S}$  values (8.8‰), despite the Monruz samples representing a significantly shorter time span (Fig. 2) and representing only two, rather than three, different animal species (Table 2). Further, unlike at Kastelhöhle-Nord, the horse and reindeer  $\delta^{34}\text{S}$  values from Monruz completely overlap with one another. Thus, while the Monruz  $\delta^{13}\text{C}$  and  $\delta^{15}\text{N}$  values suggest that horse and reindeer were occupying different ecological niches, the sulphur isotopic data suggests this was likely taking place within the same geographical region(s), and therefore under the same range of environmental and climatic

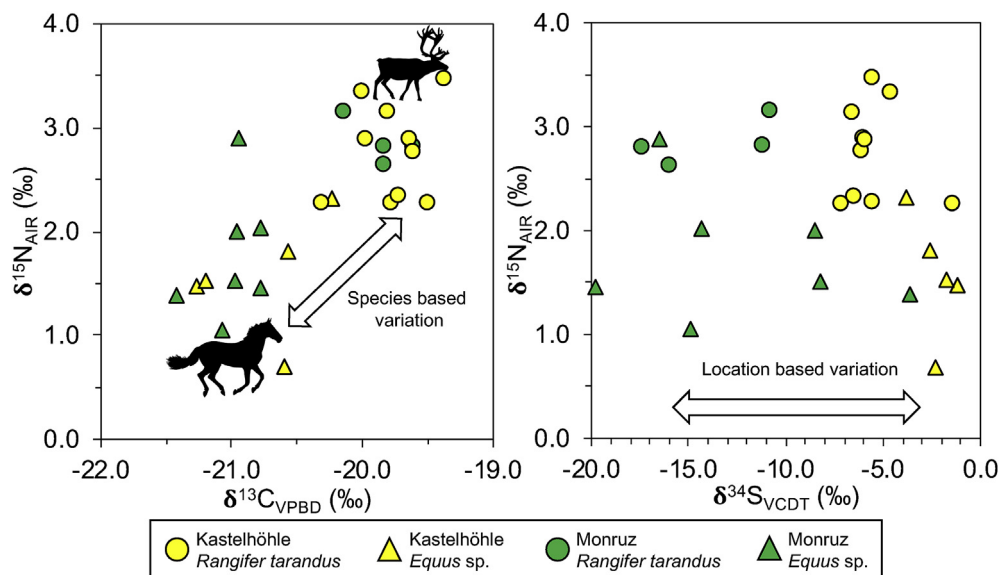


**Fig. 4.**  $\delta^{13}\text{C}$ ,  $\delta^{15}\text{N}$ , and  $\delta^{34}\text{S}$  values from reindeer (*Rangifer tarandus*, circles) and horse (*Equus* sp, triangles) from Kastelhöhle-Nord upper horizon (yellow) and Monruz (green).  $\delta^{13}\text{C}$  and  $\delta^{15}\text{N}$  values cluster by species, while  $\delta^{34}\text{S}$  values cluster by location. (For interpretation of the references to colour in this figure legend, the reader is referred to the Web version of this article.)

conditions. The large range in  $\delta^{34}\text{S}$  values could indicate both species were displaying a number of different long-distance mobility behaviours, or alternatively, could suggest a high level of environmental variability within a relatively small geographical region. As the Monruz horse produce a significantly greater range of  $\delta^{34}\text{S}$  values (16.2‰) than the reindeer (7.0‰), and unlike reindeer, horse generally do not undertake long-distance seasonal migrations, we suggest the second interpretation is more plausible. However, we recognise mobility behaviours may have differed between different environments in Late Pleistocene Europe (e.g. Bignon et al., 2005; Pelligrini et al., 2008; Pryor et al., 2016).

The isotopic composition of bioavailable sulphur is spatially variable at a range of scales. At the regional level, soil  $\delta^{34}\text{S}$  values are controlled by location-based inputs from underlying bedrock geology, sea spray and the atmosphere (Thode, 1991; Nehlich, 2015). However, Monruz and Kastelhöhle-Nord are situated far from the coast and occupy similar, relatively uniform sedimentary geologies comprised of limestone, sandstone, and clay that are unlikely to account for the range of  $\delta^{34}\text{S}$  values that we observe (Asch, 2005, Fig. 1). Other potential sources of spatial variation in  $\delta^{34}\text{S}$  values relate to more local-scale differences in soil microbial activity, influenced by soil temperature, water content and oxygen availability (Orchard and Cook, 1983; Liu et al., 2018; Nitsch et al., 2019). Indeed, paleoenvironmental records from the Swiss Plateau document a highly heterogeneous landscape existed during this period; increasing temperatures led to permafrost thaw, terrestrial landscape instability and the development of localised marshy habitats in some areas, while in other areas it facilitated vegetation development and soil stabilisation (Thew et al., 2009; Rey et al., 2017, 2019). It is these local-scale processes which we suggest are represented in the high level of variation observed in the Monruz  $\delta^{34}\text{S}$  values.

Only one result is available for the Azilian period from Monruz and Champrévevres. This was the sole sample from an Azilian context at Champrévevres to yield adequate collagen for analysis, and the only red deer sample in our data set. This sample produced  $\delta^{13}\text{C}$  and  $\delta^{15}\text{N}$  values of  $-20.6\text{‰}$  and  $2.4\text{‰}$ , respectively, which are comparable to the red deer previously analysed from the site ( $-20.6\text{‰}$  and  $3.4\text{‰}$ , Drucker et al., 2009).

### 3.3. Deglaciated versus unglaciated lateglacial landscape development

In the context of Late Pleistocene Europe, much of the spatial and temporal variation observed in herbivore bone collagen stable isotope values has been linked to soil processes, related to variations in temperature, permafrost extent and proximity to ice sheet margins (Stevens and Hedges, 2004; Stevens et al., 2008; Drucker et al., 2011b, 2012). To explore these possible drivers of the isotopic signatures, and by inference post-LGM environmental change, we compare the temporal patterns observed in fauna from neighbouring regions that had been glaciated at the LGM to those that had remained ice-free during the last glacial cycle. We combine the results of this study with those previously published from regions of Switzerland, the French Jura and Western Alps (Drucker et al., 2003, 2009; 2011a, 2011b; 2012; Stevens et al., 2008; Bocherens et al., 2011; Gröcke et al., 2017; Reade et al., 2020, Fig. 5; Supplementary Information 5). Sites are assigned to two groups based on reconstructed maximum ice extents; those in locations that remained ice-free through the LGM, and those that were ice-covered at the LGM (Campy, 1992; Bini et al., 2009; Schlüchter et al., 2010). As this analysis combines data from multiple species (*Bos/Bison*, horse, red deer, and reindeer), differences in dietary behaviours mask possible environmental interpretations from the  $\delta^{13}\text{C}$  values. Dietary ecology is also likely responsible for some of

the scatter in the  $\delta^{15}\text{N}$  data, but temporal trends are nonetheless apparent (Fig. 5). Herbivore  $\delta^{34}\text{S}$  values appear to primarily reflect the underlying environment, irrespective of differences in dietary ecology, and the different temporal patterns in the  $\delta^{34}\text{S}$  values between the two location-based groups is striking (Fig. 5).

For  $\delta^{15}\text{N}$  values, the temporal pattern of variation appears consistent between the ice-covered and ice-free areas, suggesting that the presence/absence of ice sheets and processes of deglaciation are not the direct primary influences being recorded in the signal. The most notable aspect of the record is the absence of  $\delta^{15}\text{N}$  values greater than c.  $2.5\text{‰}$  between around 15,200 and 14,800 cal. BP. As this pattern is present in samples that span a large geographical area, which is topographically and environmentally diverse, a regional-scale explanation should be sought. Low herbivore  $\delta^{15}\text{N}$  values ( $<2.5\text{‰}$ ) in Lateglacial Europe have previously been linked to environments with nutrient-poor soils, where low temperatures and the presence of permafrost impeded the soil nitrogen cycle, or to increased environmental moisture; conversely, high herbivore  $\delta^{15}\text{N}$  values ( $>5\text{‰}$ ) have been considered typical of environments where nitrogen supply is not a limiting factor to plant growth and environmental conditions do not inhibit the soil nutrient cycle (Schulze et al., 1994; Hobbie et al., 1998; Jonasson et al., 1999; Stevens and Hedges, 2004; Stark, 2007; Stevens et al., 2008; Drucker et al., 2011b, 2012; Rabanus-Wallace et al., 2017). Low  $\delta^{15}\text{N}$  values occur alongside an absence of high  $\delta^{15}\text{N}$  values at various points in the Swiss/French record shown in Fig. 5 (at c. 21,000–18,200 cal. BP, c. 15,200–14,800 cal. BP, and c. 12,200 cal. BP). However, we suggest that it is only the 15,200–14,800 cal. BP interval that can be discussed with a degree of confidence, as the exclusively low  $\delta^{15}\text{N}$  values during this time interval are clearly bounded by the presence of higher  $\delta^{15}\text{N}$  values both before and after (Fig. 5). The timing of this disappearance of  $\delta^{15}\text{N}$  values greater than c.  $2.5\text{‰}$  in the Swiss/French record broadly corresponds to the end of Heinrich Event 1 (HE1), a period of climatic cooling following the LGM, during which Alpine ice sheets expanded (Hemming, 2004; Ivy-Ochs et al., 2006). Immediately after HE1, a small but significant climatic warming is evident, although lake level data suggests annual precipitation amounts remained relatively low (Magny et al., 2006; Magny, 2013). On the Swiss Plateau localised permafrost degradation and an increase in insect and plant species diversity is evident (Thew et al., 2009; Rey et al., 2017). A similar increase in vegetation density is also evident northwest of the Jura mountains (e.g. Magny et al., 2006). It is possible that if this period corresponds to the first significant regional increase in vegetation after the LGM, such an increase even if relatively small, occurring in an already nutrient-limited environment would initially deplete nutrient availability even further. The effect of this would be a short-term decline in average plant  $\delta^{15}\text{N}$  values, followed by a rapid increase, as soils matured and nutrient cycling accelerated (Hobbie et al., 1998, 2005; Ammann et al., 2013).

Unlike the nitrogen record, sulphur isotope ratios display a significantly different pattern of change between ice-covered and ice-free areas. Ice-free areas display low  $\delta^{34}\text{S}$  values ( $<-8\text{‰}$ ) at around 23,000 cal. BP, but then remain consistently high across the deglacial period ( $>-8\text{‰}$ , except for one outlier). By contrast, in locations that were covered by ice at the LGM, low  $\delta^{34}\text{S}$  values ( $<-8\text{‰}$ ) are recorded at around 15,900 to 15,400 cal. BP, increasing to a minimum of  $-5\text{‰}$  by 15,000 cal. BP. While some of the scatter in the data can be explained by different patterns of mobility between different species, such influences cannot explain the clear location-specific differences in the temporal sulphur isotopic record. Further, while location-based geological differences may produce different absolute  $\delta^{34}\text{S}$  values, no relationship is observed between bedrock type,  $\delta^{34}\text{S}$ , and glaciated/ice-free location (Figure S4). As such, spatially and temporally variable

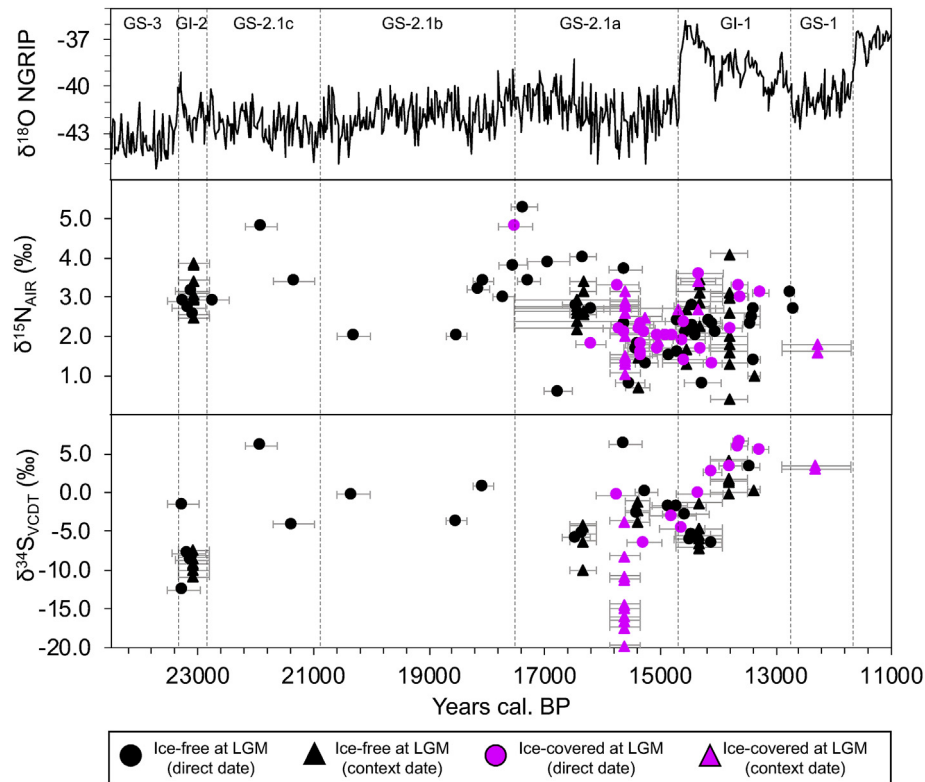


**Fig. 5.**  $\delta^{15}\text{N}$  (middle) and  $\delta^{34}\text{S}$  (bottom) isotope values from LGM and Lateglacial fauna (*Bos/Bison*, horse, red deer, reindeer) from the French and Swiss Jura, western Alps and Swiss Plateau (full data in Supplementary Information 5). INTIMATE event stratigraphy and NGRIP ice core  $\delta^{18}\text{O}$  values (top; North Greenland Ice Core Project members, 2004; Rasmussen et al., 2014). Black symbols indicate samples from locations that remained ice-free throughout the LGM, pink symbols indicate samples from locations that were ice-covered at the LGM, as displayed in Fig. 1. Circles indicate directly dated specimens (by radiocarbon), triangles indicate context dated specimens, where age has been inferred from dates on other faunal specimens from the same site/stratigraphic context. (For interpretation of the references to colour in this figure legend, the reader is referred to the Web version of this article.)

environmental parameters need to be considered. Temperature-mediated controls on soil mineralisation and volatilisation, and bacterial reduction of sulphur have been suggested to explain temporal changes in herbivore  $\delta^{34}\text{S}$  values (Drucker et al., 2011a). However, temperature change alone cannot explain the location-based differences we observe in the data, unless it was acting on a sub-regional scale. Soil maturity has also been linked to differences in herbivore sulphur isotopic ratios (Drucker et al., 2012), but this interpretation is not supported in this instance by the corresponding  $\delta^{15}\text{N}$  values.

Here, we suggest that the herbivore  $\delta^{34}\text{S}$  values reflect local soil conditions that are primarily related to hydrology and microbial activity. Plants acquire sulphur from the soil as sulphate, derived from mineral weathering and atmospheric deposition, and influenced by soil microbial action (Walker, 1957; Krouse, 1980; Robinson and Bottrell, 1997; Newton and Bottrell, 2007). Changing soil hydrological dynamics, particularly the development of water-logged environments that result in anaerobic conditions, can lead to significant differences in plant  $\delta^{34}\text{S}$  values brought about by changing bacteria-mediated fractionations (Fry et al., 1982; Trust and Fry, 1992; Groscheová et al., 2000; Nitsch et al., 2019). While the processes that govern soil  $\delta^{34}\text{S}$  in relation to changing hydrological conditions are complex and not yet fully understood (Mandernack et al., 2000; Nitsch et al., 2019), we suggest that the different pattern observed between the ice-free and recently-deglaciated regions in post-LGM Switzerland could relate to location specific hydrological dynamics, potentially related ice sheet melt, or more likely, permafrost thaw processes. Indeed, the palaeoenvironmental record from Lake Neuchâtel on the Swiss

Plateau identifies a period of permafrost thaw coinciding with considerable instability of the terrestrial landscape and localised marshy conditions, that is largely contemporaneous with the low herbivore  $\delta^{34}\text{S}$  values identified in this study at Monruz (Thew et al., 2009). By contrast, while there is greater debate about the distribution and character of permafrost north and west of the Jura, recent studies suggest that if present, it did not persist into the latter part of GS-2.1a (Renssen and Vandenberghe, 2003; Bertran et al., 2014; Vandenberghe et al., 2014). This could explain why low  $\delta^{34}\text{S}$  values during GS-2.1a are not observed in these regions.

#### 4. Conclusion

The carbon, nitrogen and sulphur isotopic ratios reported in this study attest to regionally variable environmental development in post-LGM Switzerland. Significant differences between areas that remained ice-free throughout the last glacial cycle and those that were glaciated at the LGM are identified. Deriving such information from archaeological faunal assemblages allows these environmental records to be directly related to human presence in these areas, and to subsistence and settlement strategies in such landscapes, which can more broadly inform on human behavioural ecology in peripheral settings. Our results show the post-LGM period in Switzerland and adjacent regions was characterised by diverse environmental conditions, indicating that a range of habitats and landscapes were available for humans and animals to exploit. Herbivore  $\delta^{13}\text{C}$  and  $\delta^{15}\text{N}$  values are most strongly influenced by species ecology and dietary behaviours, underpinned by environmental influences.  $\delta^{34}\text{S}$  values appear to most strongly

correspond to location-specific environmental conditions. Our results suggest that during the period of Magdalenian activity in Switzerland the Swiss Plateau was a dynamic and diverse landscape, while greater environmental stability may have existed north of the Jura Mountains.

The absence of high (>2.5‰)  $\delta^{15}\text{N}$  values between 15,200 and 14,800 cal. BP, both on the Swiss Plateau and north of the Jura, indicates a regional-scale environmental phenomenon that we suggest is related to the combination of prolonged low temperatures, limited bioavailable soil nutrients, and elevated nutrient demand from increasing vegetation cover. In contrast, low (<-8‰)  $\delta^{34}\text{S}$  values occur at different times in different locations, and we suggest that these reflect locally variable hydrological dynamics, either related to changing rates of mineral weathering and soil-bedrock interactions or to changing soil redox conditions, which govern microorganism-mediated isotopic fractionations. We suggest that either interpretation is congruous with the regionally different patterns of ice sheet melt and permafrost thaw.

### Declaration of competing interest

The authors declare that they have no known competing financial interests or personal relationships that could have appeared to influence the work reported in this paper.

### CRedit authorship contribution statement

**Hazel Reade:** Conceptualization, Data curation, Formal analysis, Investigation, Visualization, Writing - original draft. **Jennifer A. Tripp:** Formal analysis, Investigation, Writing - review & editing. **Sophy Charlton:** Data curation, Writing - review & editing. **Sonja B. Grimm:** Conceptualization, Writing - review & editing. **Denise Leesch:** Data curation, Resources, Writing - review & editing. **Werner Müller:** Data curation, Resources, Writing - review & editing. **Kerry L. Sayle:** Formal analysis, Writing - review & editing. **Alex Fensome:** Formal analysis, Writing - review & editing. **Thomas F.G. Higham:** Conceptualization, Writing - review & editing. **Ian Barnes:** Conceptualization, Writing - review & editing. **Rhiannon E. Stevens:** Conceptualization, Investigation, Supervision, Funding acquisition, Writing - review & editing.

### Acknowledgements

We thank the Archaeological Services of the cantons of Solothurn and Neuchâtel for permitting sampling of the material included in this research. We are also grateful to the Mary Rose Trust for their donation of cow ribs from the Mary Rose shipwreck, which provided known-age standard material for radiocarbon analysis. Emily Walsh is thanked for her assistance with the collagen extraction laboratory procedure. This research was funded by a European Research Council Consolidator Grant awarded to Rhiannon Stevens (grant ID: 617777).

### Appendix A. Supplementary data

Supplementary data to this article can be found online at <https://doi.org/10.1016/j.quascirev.2020.106372>.

### References

Ambrose, S.H., 1990. Preparation and characterization of bone and tooth collagen for isotopic analysis. *J. Archaeol. Sci.* 17 (4), 431–451. [https://doi.org/10.1016/0305-4403\(90\)90007-R](https://doi.org/10.1016/0305-4403(90)90007-R).  
 Ammann, B., Lotter, A.F., 1989. Late-Glacial radiocarbon- and palynostratigraphy on the Swiss Plateau. *Boreas* 18, 109–126. <https://doi.org/10.1111/j.1502-3885.1989.tb00381.x>.

Ammann, B., van Leeuwen, J.F.N., van der Knapp, W.O., Lischke, H., Heiri, O., Tinner, W., 2013. Vegetation responses to rapid warming and to minor climatic fluctuations during the Late-Glacial Interstadial (GI-1) at Gerzensee (Switzerland). *Palaeogeogr. Palaeoclimatol.* 391, 40–59. <https://doi.org/10.1016/j.palaeo.2012.07.010>.  
 Amundson, R., Austin, A.T., Schuur, E.A.G., Yoo, K., Matzke, V., Kendall, C., Uehersax, A., Brenner, D., Baisden, W.T., 2003. Global patterns of the isotopic composition of soil and plant nitrogen. *Global Biogeochem. Cycles* 17 (1), 1031. <https://doi.org/10.1029/2002GB001903>.  
 Asch, K., 2005. IGME 5000: 1:5 Million International Geological Map of Europe and Adjacent Areas. BGR (Hannover).  
 Bertran, P., Andrieux, E., Antoine, P., Coutard, S., Deschodt, L., Gardère, P., Hernandez, M., Legentil, C., Lenoble, A., Liard, M., Mercier, N., Moine, O., Sitzia, L., Van Vliet-Lanoë, B., 2014. Distribution and chronology of Pleistocene permafrost features in France: database and first results. *Boreas* 43, 699–711. <https://doi.org/10.1111/bor.12025>.  
 Bignon, O., Baylac, M., Vigne, J.-D., Eisenmann, V., 2005. Geometric morphometrics and the population diversity of Late Glacial horses in Western Europe (*Equus caballus arcelini*): phylogeographic and anthropological implications. *J. Archaeol. Sci.* 32 (2), 375–391. <https://doi.org/10.1016/j.jas.2004.02.016>.  
 Bini, A., Buoncristiani, J.-F., Couterrand, S., Ellwanger, D., Fleber, M., Florineth, D., Graf, H.R., Keller, O., Kelly, M., Schlüchter, C., Schoeneich, P., 2009. La Suisse durant le dernier maximum glaciaire (LGM) 1:500000. Federal Office of Topography Swisstopo, Switzerland.  
 Bocherens, H., Drucker, D.G., Taubald, H., 2011. Preservation of bone collagen sulphur isotopic compositions in an early Holocene river-bank archaeological site. *Palaeogeogr. Palaeoclimatol.* 310 (1–2), 32–38. <https://doi.org/10.1016/j.palaeo.2011.05.016>.  
 Bocherens, H., Drucker, D.G., Germonpré, M., Láznicková, M., Naito, W.I., Wissing, C., Brůžek, J., Oliva, M., 2015. Reconstruction of the Gravettian food-web at Předmostí I using multi-isotopic tracking ( $^{13}\text{C}$ ,  $^{15}\text{N}$ ,  $^{34}\text{S}$ ) of bone collagen. *Quat. Int.* 359–360, 211–228. <https://doi.org/10.1016/j.quaint.2014.09.044>.  
 Brock, F., Higham, T.F.G., Ditchfield, P., Bronk Ramsey, C., 2010. Current pretreatment methods for AMS radiocarbon dating at the Oxford radiocarbon accelerator unit (ORAU). *Radiocarbon* 52, 103–112. <https://doi.org/10.1017/S003822200045069>.  
 Bronk Ramsey, C., Hedges, R.E.M., 1997. Hybrid ion sources: radiocarbon measurements from microgram to milligram. *Nucl. Instr. Meth. Phys. Res. B* 123 (1–4), 539–545. [https://doi.org/10.1016/S0168-583X\(96\)00612-X](https://doi.org/10.1016/S0168-583X(96)00612-X).  
 Bronk Ramsey, C., Humm, M.J., 2000. On-line combustion of samples for AMS and ion source developments at ORAU. *Nucl. Instr. Meth. Phys. Res. B* 172, 242–246. [https://doi.org/10.1016/S0168-583X\(00\)00116-6](https://doi.org/10.1016/S0168-583X(00)00116-6).  
 Bronk Ramsey, C., Higham, T., Leach, P., 2004. Towards high-precision AMS: progress and limitations. *Radiocarbon* 46 (1), 17–24. <https://doi.org/10.1017/S0038222000039308>.  
 Campy, M., 1992. Palaeogeographical relationships between Alpine and Jura glaciers during the two last Pleistocene glaciations. *Palaeogeogr. Palaeoclimatol.* 93 (1–2), 1–12. [https://doi.org/10.1016/0031-0182\(92\)90180-D](https://doi.org/10.1016/0031-0182(92)90180-D).  
 Coope, G.R., Elias, S.A., 2000. The environment of Upper Palaeolithic (Magdalenian and Azilian) hunters at Hauterive-Champvèveres, Neuchâtel, Switzerland, interpreted from coleopteran remains. *J. Quat. Sci.* 15, 157–175. [https://doi.org/10.1002/\(SICI\)1099-1417\(200002\)15:2<157::AID-JQS478>3.0.CO;2-K](https://doi.org/10.1002/(SICI)1099-1417(200002)15:2<157::AID-JQS478>3.0.CO;2-K).  
 Craine, J.M., Elmore, A.J., Wang, L., Augusto, L., Baisden, W.T., Brookshire, E.N.J., Cramer, M.D., Hasselquist, N.J., Hobbie, E.A., Kahmen, A., Koba, K., Kranabetter, J.M., Mack, M.C., Marin-Spiotta, E., Mayor, J.R., McLauchlan, K.K., Michelsen, A., Nardoto, G.B., Oliveira, R.S., Perakis, S.S., Peri, P.L., Quesada, C.A., Richter, A., Schipper, L.A., Stevenson, B.A., Turner, B.L., Viani, R.A.G., Wanek, W., Zeller, B., 2015. Convergence of soil nitrogen isotopes across global climate gradients. *Sci. Rep.* 5, 8280. <https://doi.org/10.1038/srep08280>.  
 Cupillard, C., Magny, M., Bocherens, H., Bridault, A., Bégeot, C., Bichet, V., Bossuet, G., Drucker, D.G., Gauthier, E., Jouannic, G., Millet, L., Richard, H., Ruis, D., Ruffaldi, P., Walter-Simonnet, A.-V., 2015. Changes in ecosystems, climate and societies in the Jura Mountains between 40 and 8 ka cal BP. *Quat. Int.* 378, 40–72. <https://doi.org/10.1016/j.quaint.2014.05.032>.  
 Dee, M., Bronk Ramsey, C., 2000. Refinement of graphite target production at ORAU. *Nucl. Instrum. Meth. Phys. Res. B* 172 (1–4), 449–453. [https://doi.org/10.1016/S0168-583X\(00\)00337-2](https://doi.org/10.1016/S0168-583X(00)00337-2).  
 DeNiro, M.J., 1985. Postmortem preservation and alteration of in vivo bone collagen isotope ratios in relation to palaeodietary reconstruction. *Nature* 317, 806–809. <https://doi.org/10.1038/317806a0>.  
 Drucker, D.G., Bocherens, H., Bridault, A., Billiou, D., 2003. Carbon and nitrogen isotopic composition of red deer (*Cervus elaphus*) collagen as a tool for tracking palaeoenvironmental change during the Late-Glacial and Early Holocene in the northern Jura (France). *Palaeogeogr. Palaeoclimatol.* 195, 375–388. [https://doi.org/10.1016/S0031-0182\(03\)00366-3](https://doi.org/10.1016/S0031-0182(03)00366-3).  
 Drucker, D.G., Bridault, A., Hobson, K.A., Szuma, E., Bocherens, H., 2008. Can carbon-13 in large herbivores reflect the canopy effect in temperate and boreal ecosystems? Evidence from modern and ancient ungulates. *Palaeogeogr. Palaeoclimatol.* 266, 69–82. <https://doi.org/10.1016/j.palaeo.2008.03.020>.  
 Drucker, D.G., Bocherens, H., Billiou, D., 2009. Quelle valence écologique pour les rennes et autres cervidés au Tardiglaciaire dans les Alpes du nord et le Jura? Résultats de l'analyse des isotopes stables ( $^{13}\text{C}$ ,  $^{15}\text{N}$ ) du collagène. In: Pion, G. (Ed.), *La fin du Paléolithique supérieur dans les Alpes du nord françaises et le Jura méridional*, vol. 50. Mémoire de la Société préhistorique française, Paris, pp. 73–86.

- Drucker, D.G., Hobson, K.A., Ouellet, J.-P., Courtois, R., 2010. Influence of forage preferences and habitat use on  $^{13}\text{C}$  and  $^{15}\text{N}$  abundance in wild caribou (*Rangifer tarandus caribou*) and moos (*Alces alces*) from Canada. *Isot Environ Health S* 46 (1), 107–121. <https://doi.org/10.1080/10256010903388410>.
- Drucker, D.G., Bridault, A., Cupillard, C., Hujic, A., Bocherens, H., 2011a. Evolution of habitat and environment of red deer (*Cervus elaphus*) during the Late-glacial and early Holocene in eastern France (French Jura and the western Alps) using multi-isotope analysis ( $\delta^{13}\text{C}$ ,  $\delta^{15}\text{N}$ ,  $\delta^{18}\text{O}$ ,  $\delta^{34}\text{S}$ ) of archaeological remains. *Quat. Int.* 245, 268–278. <https://doi.org/10.1080/10256010903388410>.
- Drucker, D.G., Kind, C.J., Stephan, E., 2011b. Chronological and ecological information on Late-glacial and early Holocene reindeer from northwest Europe using radiocarbon ( $^{14}\text{C}$ ) and stable isotope ( $^{13}\text{C}$ ,  $^{15}\text{N}$ ) analysis of bone collagen: case study in southwestern Germany. *Quat. Int.* 245 (2), 218–224. <https://doi.org/10.1016/j.quaint.2011.05.007>.
- Drucker, D.G., Bridault, A., Cupillard, C., 2012. Environmental context of the Magdalenian settlement in the Jura Mountains using stable isotope tracking ( $^{13}\text{C}$ ,  $^{15}\text{N}$ ,  $^{34}\text{S}$ ) of bone collagen from reindeer (*Rangifer tarandus*). *Quat. Int.* 272–273, 268–278. <https://doi.org/10.1016/j.quaint.2012.05.040>.
- Drucker, D.G., Stevens, R.E., Germonpré, M., Sablin, M.V., Bocherens, H., 2018. Collagen stable isotopes provide insights into the end of the mammoth steppe in the central East European plains during the Epigravettian. *Quat. Res.* 90, 457–469. <https://doi.org/10.1017/qua.2018.40>.
- Fry, B., Scalan, R.S., Winters, J.K., Parker, P.L., 1982. Sulphur uptake by salt grasses, mangroves, and seagrasses in anaerobic sediments. *Geochim. Cosmochim. Acta* 46, 1121–1124. [https://doi.org/10.1016/0016-7037\(82\)90063-1](https://doi.org/10.1016/0016-7037(82)90063-1).
- Gröcke, D.R., Sauer, P.E., Bridault, A., Drucker, D.G., Germonpré, M., Bocherens, H., 2017. Hydrogen isotopes in Quaternary mammal collagen from Europe. *J. Archaeol. Sci. Rep.* 11, 12–16. <https://doi.org/10.1016/j.jasrep.2016.11.020>.
- Groscheová, H., Novák, M., Alewell, C., 2000. Changes in the  $\delta^{34}\text{S}$  ratio of pore-water sulfate in incubated Sphagnum peat. *Wetlands* 20, 62–69. [https://doi.org/10.1672/0277-5212\(2000\)020\[0062:CITSRO\]2.0.CO;2](https://doi.org/10.1672/0277-5212(2000)020[0062:CITSRO]2.0.CO;2).
- Hajdas, I., Bonani, G., Furrer, H., Mäder, A., Schoch, W., 2007. Radiocarbon chronology of the mammoth site at Niederweningen, Switzerland: results from dating bones, teeth, wood and peat. *Quat. Int.* 164–165, 98–105. <https://doi.org/10.1016/j.quaint.2006.10.007>.
- Heaton, T.H.E., 1999. Spatial, species, and temporal variations in the  $^{13}\text{C}/^{12}\text{C}$  ratios of  $\text{C}_3$  plants: implications for palaeodiet studies. *J. Archaeol. Sci.* 26 (6), 637–649. <https://doi.org/10.1006/jasc.1998.0381>.
- Hemming, S., 2004. Heinrich events: massive late Pleistocene detritus layers of the North Atlantic and their global climate imprint. *Rev. Geophys.* 42, 1–43.
- Higham, T.G., Jacobi, R.M., Bronk Ramsey, C., 2006. AMS radiocarbon dating of ancient bone using ultrafiltration. *Radiocarbon* 48 (2), 179–195. <https://doi.org/10.1017/S0033822200066388>.
- Hobbie, E., Macko, S.A., Shugart, H.H., 1998. Patterns of N dynamics and N isotopes during primary succession in Glacier Bay, Alaska. *Chem. Geol.* 152, 3–11. [https://doi.org/10.1016/S0009-2541\(98\)00092-8](https://doi.org/10.1016/S0009-2541(98)00092-8).
- Hobbie, E.A., Jumpponen, A., Trappe, J., 2005. Foliar and fungal  $^{15}\text{N}:^{14}\text{N}$  ratios reflect development of mycorrhizae and nitrogen supply during primary succession: testing analytical models. *Oecologia* 146, 258–268. <https://doi.org/10.1007/s00442-005-0208-z>.
- Ivy-Ochs, S., 2015. Glacier variations in the European Alps at the end of the last glaciation. *Cuadernos de Investigacion Geografica* 41 (2), 295–315. <https://doi.org/10.18172/cig.2750>.
- Ivy-Ochs, S., Kerschner, H., Kubik, P.W., Schlüchter, C., 2006. Glacier response in the European Alps to Heinrich event 1 cooling: the gschnitz stadial. *J. Quat. Sci.* 21, 115–130. ISSN 0267-8179.
- Ivy-Ochs, S., Schäfer, J., Kubik, P.W., Svalin, H.-A., Schlüchter, C., 2004. The timing of deglaciation on the northern Alpine foreland (Switzerland). *Eclogae Geol. Helv.* 97, 47–55. <https://doi.org/10.1007/s00015-004-1110-0>.
- Jonasson, S., Michelsen, A., Schmidt, I.K., 1999. Coupling of nutrient cycling and carbon dynamics in the Arctic; integration of soil microbial and plant processes. *Appl. Soil Ecol.* 11, 135–146. [https://doi.org/10.1016/S0929-1393\(98\)00145-0](https://doi.org/10.1016/S0929-1393(98)00145-0).
- Jones, J.R., Richards, M.P., Reade, H., de Quirós, F.B., Marin-Arroyo, A.B., 2018. Multi-isotope investigations of ungulate bones and teeth from El Castillo and Cova Lejos caves (Cantabria, Spain): implications for paleoenvironment reconstructions across the Middle-Upper Palaeolithic transition. *J. Archaeol. Sci. Rep.* 23, 1029–1042. <https://doi.org/10.1016/j.jasrep.2018.04.014>.
- Julien, M.-A., Bocherens, H., Burke, A., Drucker, D.G., Patou-Mathis, M., Krotova, O., Péan, S., 2012. Were European steppe bison migratory?  $^{18}\text{O}$ ,  $^{13}\text{C}$  and Sr intra-tooth isotopic variations applied to a palaeoethological reconstruction. *Quat. Int.* 271, 106–119. <https://doi.org/10.1016/j.quaint.2012.06.011>.
- Kohn, M.J., 2010. Carbon isotope compositions of terrestrial  $\text{C}_3$  plants as indicators of (paleo)ecology and (paleo)climate. *P Natl Acad Sci USA* 107 (46), 19691–19695. <https://doi.org/10.1073/pnas.1004933107>.
- Krouse, H.R., 1980. Sulfur isotopes in our environment. In: Fritz, P., Fontes, J.C. (Eds.), *Handbook of Environmental Isotope Geochemistry*, Amsterdam, pp. 435–471.
- Larter, N.C., Gates, C.C., 1991. Diet and habitat selection of wood bison in relation to seasonal changes in forage quantity and quality. *Can. J. Zool.* 69, 2677–2685. <https://doi.org/10.1139/z91-376>.
- Leesch, D., 1997. Hauterive-Champrevéyres. Un campement magdalénien au bord du lac de Neuchâtel. Cadre chronologique et culturel, mobilier et structures, analyse spatiale (secteur 1). *Archéologie neuchâteloise*, 19, Office et musée cantonal d'archéologie. Neuchâtel.
- Leesch, D., Müller, W., 2012. Neue Radiokarbon daten an Knochen, Zähnen und Geweih aus Magdalénien-Fundstellen der Schweiz und ihre Bedeutung für die Stellung des Magdalénien innerhalb des Spätglazials. *Jahrbuch der Archäologie Schweiz* 95, 117–126. <https://doi.org/10.5169/seals-392487>.
- Leesch, D., Cattin, M.-I., Müller, W., 2004. Témoins d'implantations magdaléniennes et azzéliennes sur la rive nord du lac de Neuchâtel. *Archéologie neuchâteloise*, 31, Office et musée cantonal d'archéologie. Neuchâtel.
- Leesch, D., Müller, W., Nielsen, E., Bullinger, J., 2012. The Magdalenian in Switzerland: Re-colonization of a newly accessible landscape. *Quat. Int.* 272–273, 191–208. <https://doi.org/10.1016/j.quaint.2012.04.010>.
- Leesch, D., Bullinger, J., Müller, W., 2019. Vivre en Suisse il y a 15000 ans. *Le Magdalénien*. Bâle, Archéologie suisse.
- Longin, R., 1971. New method of collagen extraction for radiocarbon dating. *Nature* 230 (5291), 241–242. <https://doi.org/10.1038/230241a0>.
- Lotter, A.F., 1999. Late-glacial and Holocene vegetation history and dynamics as shown by pollen and plant macrofossil analyses in annually laminated sediments from Soppensee, central Switzerland. *Veg. Hist. Archaeobotany* 8, 165–184. <https://doi.org/10.1007/BF02342718>.
- Lotter, A.F., Heiri, O., Brooks, S., van Leeuwen, J.F.N., Eicher, U., Ammann, B., 2012. Rapid summer temperature changes during Termination 1a: high-resolution multi-proxy climate reconstructions from Gerzensee (Switzerland). *Quat. Sci. Rev.* 36, 103–113. <https://doi.org/10.1016/j.quascirev.2010.06.022>.
- Liu, Y., He, N., Wen, X., Xu, L., Sun, X., Yu, G., Liang, L., Schipper, L.A., 2018. The optimum temperature of soil microbial respiration: patterns and controls. *Soil Biol. Biochem.* 121, 35–42.
- Magny, M., 2013. Climatic and environmental changes reflected by lake-level fluctuations at Gerzensee from 14,850 to 13,050 yr BP. *Palaeogeogr. Palaeoclimatol.* 391, 33–39. <https://doi.org/10.1016/j.palaeo.2012.05.003>.
- Magny, M., Aalbersberg, G., Bégeot, C., Benoit-Ruffaldi, P., Bossuet, G., Disnar, J.R., Heiri, O., Laggoun-Defarge, F., Mazier, F., Millet, L., Peyron, O., Vannière, B., Walter-Simonnet, A.V., 2006. Environmental and climatic changes in the Jura mountains (eastern France) during the Lateglacial-Holocene transition: a multiproxy record from Lake Lautey. *Quat. Sci. Rev.* 25, 414–445. <https://doi.org/10.1016/j.quascirev.2005.02.005>.
- Maier, A., 2015. *The Central European Magdalenian: Regional Diversity and Internal Variability*. Springer Netherlands, Dordrecht.
- Manderack, K.W., Lynch, L., Krouse, H.R., Morgan, M.D., 2000. Sulfur cycling in wetland peat of the New Jersey pinelands and its effect on stream water chemistry. *Geochim. Cosmochim. Acta* 64, 3949–3964. [https://doi.org/10.1016/S0016-7037\(00\)00491-9](https://doi.org/10.1016/S0016-7037(00)00491-9).
- Morel, P., Hug, B., 1996. Découverte d'un crâne tardiglaciaire de rhinocéros laineux *Coelodonta antiquitatis* (Blumenbach 1799) dans le lac de Neuchâtel, au large de Vauxmaur (NE). *Paléontologie et conservation*. *Bull. Soc. Neuchâtel. Sci. Nat.* 119, 101–110.
- Müller, W., 2013. Le site magdalénien de Monruz. 3. Acquisition, traitement et consommation des ressources animales. *Archéologie neuchâteloise*, 49, Office et musée cantonal d'archéologie. Neuchâtel.
- Müller, W., Leesch, D., 2011. Einige Neubestimmungen aus der Magdalénien-Fundstelle Hollenberg-Höhle 3 bei Arlesheim (Basel-Landschaft) und daraus folgende Überlegungen zur Nutzung der Höhle. *Jahrbuch der Archäologie Schweiz* 94, 7–20. <https://doi.org/10.5169/seals-179208>.
- Müller, W., Leesch, D., Bullinger, J., Cattin, M.-I., Plumettaz, N., 2006. Chasse, habitats et rythme des déplacements: réflexions à partir des campements magdaléniens de Champrevéyres et Monruz (Neuchâtel, Suisse). *Bull. Soc. Prehist. Fr.* 103 (4), 741–752.
- Napierala, H., 2008. Die Tierknochen aus dem Kesslerloch. Neubearbeitung der paläolithischen Fauna. Beiträge zur Schaffhauser Archäologie 2. Baudepartement des Kantons Schaffhausen. Kantonsarchäologie, Schaffhausen.
- Nehlich, O., 2015. The application of sulphur isotope analyses in archaeological research: a review. *Earth Sci. Rev.* 142, 1–17. <https://doi.org/10.1016/j.earscirev.2014.12.002>.
- Nehlich, O., Richards, M.P., 2009. Establishing quality criteria for sulphur isotope analysis of archaeological bone collagen. *Archaeol. Anthropol. Sci.* 1, 59–75. <https://doi.org/10.1007/s12520-009-0003-6>.
- Newton, R., Bottrell, S., 2007. Stable isotopes of carbon and sulphur as indicators of environmental change: past and present. *J. Geol. Soc.* 164, 691–708. <https://doi.org/10.1144/0016-76492006-101>.
- Nielsen, E.H., 2013. Response of the Lateglacial fauna to climatic change. *Palaeogeogr. Palaeoclimatol.* 391, 99–110. <https://doi.org/10.1016/j.palaeo.2012.12.012>.
- Nitsch, E.K., Lamb, A.L., Heaton, T.H.E., Vaiglova, P., Fraser, R., Hartman, G., Moreno-Jiménez, López-Piñero, A., Peña-Abades, D., Fairbairn, A., Eriksen, J., Bogaard, A., 2019. The preservation and interpretation of  $\delta^{34}\text{S}$  values in charred archaeological remains. *Archaeometry* 61 (1), 161–178. <https://doi.org/10.1111/arcm.12388>.
- Orchard, V.A., Cook, F.J., 1983. Relationship between soil respiration and soil moisture. *Soil Biol. Biochem.* 15 (4), 447–453.
- Pelligrini, M., Donahue, R.E., Chenery, C., Exans, J., Lee-Thorp, J., Montgomery, J., Mussi, M., 2008. Faunal migration in late-glacial central Italy: implications for human resource exploitation. *Rapid Commun. Mass Spectrom.* 22 (11), 1714–1726. <https://doi.org/10.1002/rcm.3521>.
- Pryor, A.J., Stevens, R.E., Pike, A.W.G., 2016. Seasonal mobility of the adult horse killed by hunters at Klementowice. In: Wisniewski, T. (Ed.), *Klementowice. A Magdalenian Site in Eastern Poland*. Lublin, PL. Instytut Archeologii Uniwersytetu Marie Curie Skłodowskiej, pp. 298–304.
- Rabanus-Wallace, M., Wooller, M., Zazula, G., Shute, E., Jahren, A.H., Kosintsev, P., Burns, J.A., Breen, J., Llamas, B., Cooper, A., 2017. Megafaunal isotopes reveal role of increased moisture on rangeland during late Pleistocene extinctions. *Nat. Ecol.*

- Evol 1, 0125. <https://doi.org/10.1038/s41559-017-0125>.
- Rasmussen, S.O., Bigler, M., Blockley, S.P., Blunier, T., Buchardt, S.L., Clausen, H.B., Cvijanovic, I., Dahl-Jensen, D., Johnsen, S.J., Fischer, H., Gkins, V., Guillevic, M., Hoek, W.Z., Lowe, J.J., Pedro, J.B., Popp, T., Seierstad, I.K., Steffensen, J.P., Svensson, A.M., Vallelonga, P., Vinther, B.M., Walker, M.J.C., Wheatley, J.J., Winstrup, M., 2014. A stratigraphic framework for abrupt climatic changes during the Last Glacial period based on three synchronized Greenland ice-core records: refining and extending the INTIMATE event stratigraphy. *Quat. Sci. Rev.* 106, 14–28. <https://doi.org/10.1016/j.quascirev.2014.09.007>.
- Reade, H., Tripp, J.A., Charlton, S., Grimm, S.B., Sayle, K.L., Fensome, A., Higham, T.F.G., Barnes, I., Stevens, R.E.S., 2020. Radiocarbon chronology and environmental context of Last Glacial Maximum human occupation in Switzerland. *Sci. Rep.* 10, 4694. <https://doi.org/10.1038/s41598-020-61448-7>.
- Renssen, H., Vandenberghe, J., 2003. Investigation of the relationship between permafrost distribution in NW Europe and extensive winter sea-ice cover in the North Atlantic Ocean during the cold phases of the Last Glaciation. *Quat. Sci. Rev.* 22, 209–223. [https://doi.org/10.1016/S0277-3791\(02\)00190-7](https://doi.org/10.1016/S0277-3791(02)00190-7).
- Rey, F., Gobet, E., van Leeuwen, J.F.N., Gilli, A., van Raden, U.J., Hafner, A., Wey, O., Rhiner, J., Schmocker, D., Zünd, J., Tinner, W., 2017. Vegetational and agricultural dynamics at Burgäschisee (Swiss Plateau) recorded for 18,700 years by multi-proxy evidence from partly varved sediments. *Veg. Hist. Archaeobotany* 26 (6), 571–586. <https://doi.org/10.1007/s00334-017-0635-x>.
- Rey, F., Gobet, E., Schwörer, C., Hafner, A., Tinner, W., 2019. Climate impacts on deglaciation and vegetation dynamics since the last glacial maximum at moossee (Switzerland). submitted for publication *Clim. Past Discuss.* <https://doi.org/10.5194/cp-2019-121>.
- Robinson, B.W., Bottrell, S.H., 1997. Discrimination of sulphate sources in pristine and polluted New Zealand river catchments using stable isotopes. *Appl. Geochem.* 12, 305–319. [https://doi.org/10.1016/S0883-2927\(96\)00070-4](https://doi.org/10.1016/S0883-2927(96)00070-4).
- Sayle, K.L., Brodie, C.R., Cook, G.T., Hamilton, W.D., 2019. Sequential measurement of  $\delta^{15}\text{N}$ ,  $\delta^{13}\text{C}$  and  $\delta^{34}\text{S}$  values in archaeological bone collagen at the Scottish Universities Environmental Research centre (SUERC): a new analytical frontier. *Rapid Commun. Mass Spectrom.* 33, 1258–1266. <https://doi.org/10.1002/rcm.8462>.
- Schlüchter, C., Bini, A., Buoncristiani, J.F., Couterand, S., Ellwanger, D., Felber, M., Florineth, D., Graf, H.R., Keller, O., Kelly, M., Schoeneich, P., 2010. Die Schweiz während des letzteiszeitlichen Maximum (LGM) 1:500 000. Bundesamt für Landestopografie Swisstopo, Wabern.
- Schulze, E.D., Chapin, F.S., Gebauer, G., 1994. Nitrogen nutrition and isotope differences among life forms at the Northern Treeline of Alaska. *Oecologia* 100, 406–412. <https://doi.org/10.1007/BF00317862>.
- Schweizer, T., Schmid, E., Bay, R., 1959. Die «Kastelhöhle» im Kaltbrunnental, Gemeinde Himmelried (Solothurn). *Jahrbuch für Solothurnische Geschichte* 32, 1–88.
- Sealy, J., Johnson, M., Richards, M.P., Nehlich, O., 2014. Comparison of two methods of extracting bone collagen for stable carbon and nitrogen analysis: comparing whole bone demineralization with gelatinization and ultrafiltration. *J. Archaeol. Sci.* 47, 64–69. <https://doi.org/10.1016/j.jas.2014.04.011>.
- Stark, S., 2007. Nutrient cycling in the tundra. In: Marschner, P., Rengel, Z. (Eds.), *Nutrient Cycling in Terrestrial Ecosystems*, vol. 10. Soil Biology, Springer, Berlin.
- Stevens, R.E., Hedges, R.E.M., 2004. Carbon and nitrogen stable isotope analysis of northwest European horse bone and tooth collagen, 40,000 BP-present: palaeoclimatic interpretations. *Quat. Sci. Rev.* 23, 977–991. <https://doi.org/10.1016/j.quascirev.2003.06.024>.
- Stevens, R.E., Jacobi, R., Street, M., Germonpré, M., Conard, N.J., Münzel, S.C., Hedges, R.E.M., 2008. Nitrogen isotope analyses of reindeer (*Rangifer tarandus*), 45,000 BP to 9,000 BP: palaeoenvironmental reconstructions. *Palaeogeogr. Palaeoclimatol.* 262, 32–45. <https://doi.org/10.1016/j.palaeo.2008.01.019>.
- Stevens, R.E., Hermoso-Buxán, X.L., Marín-Arroyo, A.B., González-Morales, M.R., Straus, L.G., 2014. Investigation of Late Pleistocene and Early Holocene palaeoenvironmental change at El Mirón cave (Cantabria, Spain): insights from carbon and nitrogen isotope analyses of red deer. *Palaeogeogr. Palaeoclimatol.* 414, 46–60. <https://doi.org/10.1016/j.palaeo.2014.05.049>.
- Szpak, P., Metcalfe, J.Z., Macdonald, R.A., 2017. Best practices for calibrating and reporting stable isotope measurements in archaeology. *J. Archaeol. Sci. Rep.* 13, 609–616. <https://doi.org/10.1016/j.jasrep.2017.05.007>.
- Terberger, T., Street, M., 2002. Hiatus or continuity? New results for the question of pleniglacial settlement in central Europe. *Antiquity* 76, 691–698. <https://doi.org/10.1017/S0003598X00091134>.
- Thew, N., Hadorn, P., Coope, R., 2009. Hauterive/Rouges-Terres. Reconstruction of Upper Palaeolithic and Early Mesolithic Natural Environments. *Archéologie Neuchâteloise*, 44. Office et musée cantonal d'archéologie, Neuchâtel.
- Thode, H.G., 1991. Sulfur isotopes in nature and the environment: an overview. In: Krouse, H.R., Grinenko, V.A. (Eds.), *Stable Isotopes: Natural and Anthropogenic Sulfur in the Environment*. John Wiley and Sons, Chichester, pp. 1–26.
- Trust, B.A., Fry, B., 1992. Stable sulphur isotopes in plants: a review. *Plant Cell Environ.* 15, 1105–1110. <https://doi.org/10.1111/j.1365-3040.1992.tb01661.x>.
- Vandenberghe, J., French, H.M., Gorbunov, A., Marchenko, S., Velichko, A.A., Jin, H., Cui, Z., Zhang, T., Wan, X., 2014. The Last Permafrost Maximum (LPM) map of the Northern Hemisphere: permafrost extent and mean annual air temperatures, 25–17 ka BP. *Boreas* 43, 652–666. <https://doi.org/10.1111/bor.12070>.
- Walker, R.W., 1957. The sulfur cycle in grassland soils. *Grass Forage Sci.* 12, 10–18. <https://doi.org/10.1111/j.1365-2494.1957.tb00086.x>.
- Wehrli, M., Tinner, W., Ammann, B., 2007. 16,000 years of vegetation and settlement history from Egelsee (Menzingen, central Switzerland). *Holocene* 17 (6), 747–761. <https://doi.org/10.1177/0959683607080515>.
- Weniger, G.-C., 1989. The Magdalenian in western central Europe: settlement pattern and regionality. *J. World Prehist.* 3 (3), 323–372. <https://doi.org/10.1007/BF00975326>.
- Wißing, C., Rougier, H., Baumann, C., Comeyne, A., Crevecoeur, I., Drucker, D.G., Gaudzinski-Windheuser, S., Germonpré, M., Gómez-Olivencia, A., Krause, J., Matthies, T., Naito, Y.L., Posth, C., Semal, P., Street, M., Bocherens, H., 2019. Stable isotopes reveal patterns of diet and mobility in the last Neandertals and first modern humans in Europe. *Sci. Rep.* 9, 4433. <https://doi.org/10.1038/s41598-019-41033-3>.
- Wood, R.E., Bronk Ramsey, C., Higham, T.G., 2010. Refining background corrections for radiocarbon dating of bone collagen at ORAU. *Radiocarbon* 52 (2), 600–611.

## References appearing only in figures and tables:

- Becker, D., Verheul, J., Zickel, M., Willmes, C., 2015. LGM Palaeoenvironment of Europe - Map. CRC806-Database. <https://doi.org/10.5880/SFB806.15>.
- Bodu, P., Debout, G., Dumarcay, G., Leesch, D., Valentin, B., 2009. Révision de la chronologie magdalénienne dans le Bassin parisien et alentours: nouveaux résultats. In: Valentin, B. (Ed.), *Paléolithique final et Mésolithique dans le Bassin parisien et ses marges. Habitats, sociétés et environnements, Projet collectif de recherche, Programmes P7, P8 et P10 Rapport d'activités pour 2009*, Paris, pp. 91–99.
- Bronk Ramsey, C., 2017. Methods for summarizing radiocarbon datasets. *Radiocarbon* 59 (6), 1809–1833.
- North Greenland Ice Core Project members, 2004. High-resolution record of Northern Hemisphere climate extending into the last interglacial period. *Nature* 431 (7005), 147–151.
- Reimer, P.J., Bard, E., Bayliss, A., Beck, J.W., Blackwell, P.G., Ramsey, C.B., Buck, C.E., Cheng, H., Edwards, R.L., Friedrich, M., Grootes, P.M., Guilderson, T.P., Hafflason, H., Hajdas, I., Hatté, C., Heaton, T.J., Hoffmann, D.L., Hogg, A.G., Hughen, K.A., Kaiser, K.F., Kromer, B., Manning, S.W., Niu, M., Reimer, R.W., Richards, D.A., Scott, E.M., Southon, J.R., Staff, R.A., Turney, C.S.M., van der Plicht, J., 2013. IntCal13 and Marine13 radiocarbon age calibration curves 0–50,000 Years cal BP. *Radiocarbon* 55 (4), 1869–1887.